# Laser-Rate-Equation Description of Optomechanical Oscillators

J. B. Khurgin,[1] M. W. Pruessner,[2] T. H. Stievater,[2] and W. S. Rabinovich[2]
[1]*Johns Hopkins University, Baltimore Maryland 21218, USA*
[2]*Naval Research Laboratory, Washington, D.C. 20375, USA*
(Received 6 September 2011; published 31 May 2012)

We develop a set of laser rate equations that accurately describes mechanical amplification in optomechanical oscillators driven by photothermal or radiation pressure forces. In the process we introduce a set of parameters describing gain, stored energy, slope efficiency, and saturation power of the mechanical laser. We identify the three-phonon parametric interactions as a microscopic mechanism enabling self-oscillation. Our theory shows remarkable agreement with our experimental data, demonstrating that optomechanical self-oscillation is essentially a ''phonon lasing'' process in which an optical pump generates coherent acoustic phonons.

DOI: 10.1103/PhysRevLett.108.223904 PACS numbers: 42.55.−f, 07.10.Cm, 42.65.−k

Cavity optomechanics enables resonantly enhanced light to exert forces on small mechanical objects with high quality mechanical (acoustic) resonances [1–3]. If the mechanical object comprises the whole resonant cavity (as in microdisks and toroids [4]) or a part of it (as in Fabry-Perot cavities [5]), then a feedback backaction mechanism is established that enables external optical control of both frequency and amplitude of the mechanical oscillations. The frequency and amplitude changes are usually achieved by tuning the optical wavelength around the resonance, and, from a practical point of view, the control of amplitude has been the focus of attention of many groups. Reducing the vibration amplitude of a mechanical mode can be thought of as reducing its effective temperature, thereby making it a highly sensitive detector of various external forces.

While most research has concentrated on achieving optomechanical cooling [6–8], it has also been demonstrated that by simply changing the sign of the detuning (i.e., tuning the wavelength either red- or blueshifted compared to the cavity optical resonance) an opposite effect can be achieved. The resulting large increase in the amplitude of mechanical oscillations with optical power is accompanied by the reduction of the linewidth of these oscillations. It has also been shown in various optomechanical schemes that beyond a certain threshold power self-sustained mechanical oscillations materialize [9,10] leading a number of researchers to demonstrate mechanical or phonon lasing [11,12]. However, explanations of above-threshold optomechanical oscillation as phonon lasing have not, until this Letter, described either the ''gain'' or ''emission'' in the context of energy balance. Lasing generally comprises an act of stimulated emission of coherent bosons occurring in the gain medium and is typically described by a set of two coupled rate (balance) equations: one for the gain (or population inversion) and the other for the bosons in the resonant mode [13–15]. Within this model the onset of lasing is always characterized by the twin telltale signs of rapid growth of oscillating power combined with the collapse of the linewidth. While these signs have been observed before for optomechanical oscillators [5,7,9], they have not been explained in the framework of balance equations and no customary laser terms, such as gain, population inversion, saturation power and slope efficiency have been formulated for optomechanical oscillators.

In this Letter, we develop a set of mechanical laser rate equations with identifiable parameters describing gain, stored energy, slope efficiency, and saturation power. Our theory shows remarkable agreement with our experimental data in terms of power and linewidth, demonstrating that optomechanical self-oscillation is essentially a ''lasing'' process in which an optical pump generates coherent acoustic phonons. We consider a silicon-on-insulator micro-optomechanical oscillator [16] consisting of a suspended silicon microbridge that is clamped at both ends [Fig. 1(a)]. The $SiO_2$ layer has been etched from underneath the microbridge so that it is otherwise free to vibrate. Perpendicular to and intersecting the microbridge is a rib

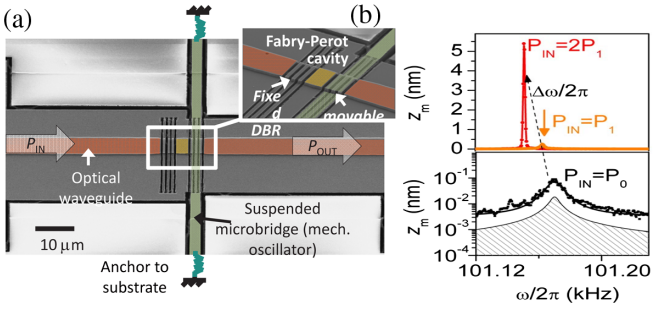


FIG. 1 (color online). (a) Fabricated device and schematic showing micromechanical oscillator and optical Fabry-Perot cavity (b) Measured *device 1* displacement amplitude, $z_m$, for various optical powers, $P_0 = 13\ \mu$W and $P_1 = 206\ \mu$W. The shaded curve is the calculated thermal noise spectrum. Above threshold ($P_{in} = 2P_1$) the oscillation amplitude increases 20× compared to below threshold ($P_{in} = P_1$).

 

waveguide into which two sets of $\lambda/4$ air trenches have been etched. Each set of air trenches forms a high-reflectivity ($R > 98\%$) distributed Bragg reflector (DBR), which together form a Fabry-Perot microcavity. One of the DBR's is fixed while the second is etched into the center of the vibrating microbridge. Any in-plane microbridge oscillation therefore modulates the position of the second DBR and modulates the Fabry-Perot microcavity transmittance.

We perform all our measurements with the laser wavelength red-detuned with respect to the Fabry-Perot optical resonance. In Fig. 1(b), we show several mechanical resonance spectra measured in vacuum ($P \sim 20$ m Torr) using the experimental setup described in [16]. At low optical power ($P_{\text{in}} = 13\ \mu$W) the measured spectrum is just above the calculated thermal noise floor indicating a minimal optomechanical interaction. As we increase the power ($P_{\text{in}} = 206\ \mu$W) the linewidth narrows and the amplitude increases linearly. However, a further increase in optical power ($P_{\text{in}} = 412\ \mu$W) leads to a strong nonlinear increase in oscillation amplitude, indicating a threshold condition. The accompanying frequency shift ($\Delta\omega$) is the result of radiation pressure [16] while the threshold condition is photothermal in nature as is explained below. The simultaneous presence of photothermal and radiation pressure forces acting in opposite directions at vastly different time scales enables us to separate their effects in a straightforward manner [16] and we focus mainly on the photothermal force here as it relates to the threshold condition.

We now derive a set of two optomechanical laser rate equations. Since the "output power" of a mechanical laser is related to the vibration amplitude and the gain to the temperature rise, it is the equations for these two variables that serve as a basis for our derivations. The position of the beam has both steady-state and oscillating components, $z = \bar{z}_0 + \frac{1}{2} z_m \exp(j\omega t) + \text{c.c.}$ where $z_m$ is the slow-variable amplitude. A change in the optical cavity length causes a change in the optical power at the DBR etched into the microbridge. This power also has two components, $\Delta P = \Delta\bar{P} + \frac{1}{2} P_m \exp(j\omega t) + \text{c.c.}$ which causes the temperature to rise relative to the ambient temperature $\Delta T = \Delta\bar{T} + \frac{1}{2} T_m \exp(j\omega t) + \text{c.c.}$. The rise in the amplitude of temperature oscillations is determined from $dT_m/dt = -(j\omega + 1/\tau_t)T_m + \alpha R_t P_m/\tau_t$ where $\alpha$ is the total absorption in the beam, $R_t$ is the thermal resistance and $\tau_t$ is the thermal relaxation time. The relationship between $P_m$ and $z_m$ is determined by the derivative of the power inside the cavity with respect to the change in optical length (that is, the derivative of our cavity line shape). To maximize the derivative, the laser wavelength must be shifted from the resonance by a small amount, which for a Fabry-Perot cavity with finesse $F$ and $Q$-factor $Q_{\text{opt}}$ can be found as $\Delta\lambda \approx \lambda/(2\sqrt{3}Q_{\text{opt}})$. This causes the second derivative to vanish and only the first and third order derivatives may be kept in a series expansion, with the values equal to $P' = z_1^{-1} P_{\text{in}} \approx \mp(3F)^2/(\pi n_{\text{Si}}\sqrt{3}) T_{\text{cav}}^{1/2} \lambda^{-1} P_{\text{in}}$ and $P''' = z_3^{-3} P_{\text{in}} \approx \pm 8(3F)^4/(\pi\sqrt{3}) T_{\text{cav}}^{1/2} \lambda^{-3} n_{\text{Si}}^{-3} P_{\text{in}}$ respectively, where $T_{\text{cav}}$ is the cavity transmission at resonance, $n_{\text{Si}} = 3.48$ is the effective refractive index of the Si waveguide, and $P_{\text{in}}$ is the waveguide optical power incident on the cavity. One obtains $P_m = P_{\text{in}}(z_m/z_1)(1 - z_m^2/z_{\text{sat}}^2)$, where we have introduced the saturation amplitude $z_{\text{sat}} = \sqrt{-z_3^3/z_1} \approx \lambda n_{\text{Si}}/3F$. Assuming that the heating is nearly adiabatic, i.e., $d/dt \ll \omega_0, \tau_t^{-1}$, we obtain

$$\frac{dT_m'(t)}{dt} + \frac{T_m'(t)}{\tau_t}(1 + \omega^2\tau_t^2) = \frac{1}{\tau_t}\alpha R_t P_{\text{in}}(t)\frac{z_m}{z_1}\left[1 - \frac{z_m^2}{z_{\text{sat}}^2}\right],$$
$$\frac{dT_m''(t)}{dt} + \frac{T_m''(t)}{\tau_t}(1 + \omega^2\tau_t^2) = -\omega\alpha R_t P_{\text{in}}(t)\frac{z_m}{z_1}\left[1 - \frac{z_m^2}{z_{\text{sat}}^2}\right], \tag{1}$$

for the real and imaginary (quadrature) components of temperature. Details of the derivation are shown in the Supplemental Material [17]. Now, the equilibrium position of the beam, $z_0$, is modified as the beam expands due to the increase in temperature and can be written as $z_0 = \bar{z}_0 + \frac{1}{2}(\frac{\partial z}{\partial T}) T_m \exp(j\omega t) + \text{c.c}$, where $(\frac{\partial z}{\partial T})$ is a thermal-displacement gain coefficient that relates the beam displacement to changes in temperature via thermal expansion [16]. Inserting that into a damped mechanical oscillator equation $d^2z/dt^2 + \gamma dz/dt = -\omega_0^2[z - z_0(t)]$ yields for the slowly variable amplitude of oscillations

$$\frac{dz_m}{dt} = -\frac{\gamma}{2} z_m - \frac{j}{2\omega}\left(\omega^2 - \omega_0^2 - \omega_0^2 \frac{dz}{dT}\frac{T_m'}{z_m}\right) z_m - \frac{1}{2\omega}\omega_0^2 \frac{dz}{dT}\frac{T_m''}{z_m} z_m. \tag{2}$$

The first term describes the damping, the term in parentheses is the observed resonant frequency shift [16,18] that can be also thought of as a frequency pulling in a conventional laser theory ([13], Eq. 12.13), while the last term describes the gain. Note that only the quadrature component of $T_m$ contributes to the gain, which is precisely the 90 degree phase shift occurring in optical parametric oscillators [13]—an analogy explored below. Finally, we obtain for the square of the amplitude

$$\frac{dz_m^2}{dt} = z_m \frac{dz_m^*}{dt} + z_m^* \frac{dz_m}{dt} = -\gamma z_m^2 - \frac{1}{\omega}\omega_0^2 \frac{dh}{dT}\frac{T''}{z_m} z_m^2 = [g(z_m) - \gamma] z_m^2, \tag{3}$$

where we have introduced our gain (per unit of time) $g = -(\omega_0^2/\omega)(dz/dT)T''/z_m$. The rate equation for the gain is then obtained from (1) as

$$\frac{dg}{dt} + \frac{g}{\tau_t'} = \frac{g_0}{\tau_t'}(1 - z_m^2/z_{\text{sat}}^2), \tag{4}$$

where the unsaturated gain is $g_0(P_{\text{in}}) = \alpha(dz/dT)R_t P_{\text{in}}(t) z_1^{-1} \omega^2 \tau_t'$, and the modified thermal

relaxation time is $\tau_t' = \tau_t/(1+\omega^2\tau_t^2)$. Equations (3) and (4) represent our main result: a coupled set of equations for gain and oscillating power in an optomechanical system.

Equations (3) and (4) and can be rewritten as a set of standard laser rate equations (Eq. 13.43 in [13]) and to better describe the energy balance. We introduce the energy of mechanical vibrations, $U_m = \frac{1}{2}m\omega^2 z_m^2$, its saturation value, $U_{\rm sat} = \frac{1}{2}m\omega^2 z_{\rm sat}^2$, and another variable, the stored energy of phase-locked thermal phonons that are available for lasing $U_{\rm st} = g\tau_t' U_{\rm sat}$, whose unsaturated value is $U_{\rm st,0} = g_0\tau_t' U_{\rm sat}$. We also include the thermal noise power $P_N = \gamma kT/2$ in the equation to obtain

$$\begin{aligned}\frac{dU_{\rm st}}{dt} &= \frac{U_{\rm st,0}}{\tau_t'}\left[1-\frac{U_m}{U_{\rm sat}}\right] - \frac{U_{\rm st}}{\tau_t'},\\ \frac{dU_m}{dt} &= \left[\frac{U_{\rm st}}{\tau_t' U_{\rm sat}} - \gamma\right]U_m + P_N.\end{aligned} \tag{5}$$

For the relatively weak vibrations $z_m \ll z_{\rm sat}$ the first of Eqs. (5) can be approximated as

$$\frac{dU_{\rm st}}{dt} = \eta_p P_{\rm in} - \frac{U_{\rm st}}{\tau_t'} - \frac{U_{\rm st}}{\tau_t'}\frac{U_m}{U_{\rm sat}}, \tag{6}$$

where we have introduced the pumping efficiency $\eta_p = \frac{U_{\rm st,0}}{P_{\rm in}\tau_t'} = \frac{\omega T_{\rm cav}^{1/2}}{2\pi\sqrt{3}}\alpha R_t\frac{dz}{dT}K_{\rm eff}\lambda n_{\rm Si}\omega\tau_t'$ and $K_{\rm eff} = m_{\rm eff}\omega_0^2$ is the effective spring coefficient. The stimulated emission term $U_{\rm st}U_m/U_{\rm sat}\tau_t'$ appears in both equations for stored and released energies with opposite signs indicating perfect energy balance as the energy is transferred from thermal phonons in all acoustic modes into coherent phonons in a single resonant mechanical mode. Also, note that neither $U_{\rm st,0}$ nor $\eta_p$ depend on cavity finesse, which is consistent because they basically represent the area under the optical force curve.

Next, we divide all the energies by a phonon energy $\hbar\omega$ to obtain a standard set of Statz–de Mars [14,15] balance equations

$$\begin{aligned}\frac{dN_{\rm st}}{dt} &= \frac{N_{\rm st,0}}{\tau_t'} - \frac{N_{\rm st}}{\tau_t'}\left[1+\frac{n_m}{N_{\rm sat}}\right],\\ \frac{dn_m}{dt} &= \left[\frac{N_{\rm st}}{\tau_t' N_{\rm sat}} - \gamma\right]n_m + \gamma\frac{kT}{2\hbar\omega},\end{aligned} \tag{7}$$

with $n_m$ being the number of coherent phonons, $N_{\rm st}$ playing the role of population inversion, and $(\tau_t' N_{\rm sat})^{-1}$ being the equivalent of stimulated emission coefficient. One difference between the rate Eqs. (7) and the standard laser equations is that the noise term is of a thermal nature and thus appears to be classical. However, this is simply the approximation of a fully quantum Bose-Einstein distribution term for the case of $kT \gg \hbar\omega$ and is not related to the fact that our quanta are phonons and not photons.

We introduce the threshold value of stored energy, $U_{\rm st,th} = \gamma\tau_t' U_{\rm sat}$, and the threshold pump power

$$P_{\rm th} = U_{\rm st,th}/\eta_p\tau_t' \approx \frac{0.62}{Q_m F^2 T_{\rm cav}^{1/2}}\frac{1+\omega^2\tau_t^2}{\omega\tau_t}\frac{\lambda n_{\rm Si}}{\alpha(dz/dT)R_t}, \tag{8}$$

where $Q_m$ is the $Q$ factor of mechanical oscillation. Note that using our theory, we could have considered the case when the optical force is due to radiation pressure to obtain a much higher value of the threshold,

$$\begin{aligned}P_{\rm th,rad} &\approx \frac{0.62}{Q_m F^2}\frac{1+\omega^2\tau_c^2}{\omega\tau_c}\lambda n_{\rm Si} c m_{\rm eff}\omega^2\\ &\approx \frac{0.62}{Q_m Q_{\rm opt} F^2} m_{\rm eff} n_{\rm Si} c^2\omega,\end{aligned} \tag{9}$$

because in place of the thermal time $\tau_t$ a much shorter cavity lifetime $\tau_c \sim Q_{\rm opt}\lambda/c$ would have been used, consistent with [9].

To obtain input-output curves it is convenient to define all the relevant energies and power as $u_{\rm st} = U_{\rm st}/U_{\rm st,th}$, $u_m = U_m/U_{\rm sat}$, and $p_{\rm in} = P_{\rm in}/P_{\rm th}$ to obtain dimensionless laser equations identical to the ones in [14,15]:

$$\begin{aligned}\frac{du_{\rm st}}{dt} &= \frac{1}{\tau_t}[p_{\rm in}(1-u_m) - u_{\rm st}]\frac{du_m}{dt}\\ &= \gamma(u_{\rm st}-1)u_m + \gamma\frac{kT}{2U_{\rm sat}}.\end{aligned} \tag{10}$$

Above threshold, the "population inversion" gets clamped at a threshold $u_{\rm st} = 1$ and the steady-state solution for the energy of mechanical oscillation can be found as $u_m = (p_{\rm in}-1)/p_{\rm in}$ with the term in the denominator indicating the phenomenon of "gain compression" [19]. In real units we obtain for the output power dissipated by the mechanical beam and otherwise available to perform work $P_{\rm out} = \gamma U_m = \eta_p(P_{\rm in}/P_{\rm th})^{-1}(P_{\rm in}-P_{\rm th})$ with the slope efficiency being equal to the pump efficiency modified by the gain compression term $(P_{\rm in}/P_{\rm th})^{-1}$. Using the second equation in (10) we can write for the linewidth:

$$\gamma_{\rm eff} = \gamma(1-u_{\rm st}) \approx \begin{cases}\gamma(1-P_{\rm in}/P_{\rm th}) & P_{\rm in} < P_{\rm th}\\ \gamma^2\frac{kT}{2P_{\rm out}} & P_{\rm in} > P_{\rm th}\end{cases}. \tag{11}$$

We have performed lasing measurements for two devices for comparison with our model. *Device 1* (*device 2*) has the following properties: $\omega_0/2\pi = 101$ kHz (101 kHz), $\gamma/2\pi = 5.54$ Hz (3.98 Hz), $Q_m = 1.89\times10^4$, $(2.79\times10^4)$, $F = 140$ (380), $T_{\rm cav} = 4.7\%$ (4.1%), $z_1^{-1} = 1.6/\text{nm}$, $(7.7/\text{nm})$, and $z_{\rm sat} = 12.9$ nm (4.8 nm). The dominant thermal time constant for these devices is estimated (via finite-element structural-mechanical modeling) to be 3.0 $\mu$s (dominated by heat flow out of the DBR silicon slabs) [16]. The corresponding expansion term was estimated to be $R_t(dz/dT) = 18.3\times10^3$ nm/W [16]. We use a transfer matrix model to estimate the field penetration and thereby absorption into the DBR slabs [16]. With the Si

absorption coefficient equal to $\alpha_{Si} = 1.6\ \mathrm{cm}^{-1}$ we obtain $\alpha \approx 3.2 \times 10^{-5}$ and find the threshold powers for our two devices as 268 $\mu$W and 31.1 $\mu$W, respectively. We use the calculated result for the spring constant $K_{\mathrm{eff}} = 2.75 \times 10^{-9}$ N/nm to obtain saturation powers $P_{\mathrm{sat}} = \gamma U_{\mathrm{sat}}$ equal to 7.98 fW and 0.86 fW, respectively, with slope efficiencies of $3.1 \times 10^{-11}$ and $3.6 \times 10^{-11}$, respectively.

The results of our calculation are plotted in Fig. 2 with no fitting parameters used, along with our experimental results for *device 1* and *device 2*.. Our instrument bandwidth is 1 Hz, which is deconvolved from our measured Lorentzian lines hapes. The experimental output powers are found by first converting our measured output laser oscillation amplitude into an oscillating displacement amplitude ($z_m$ as in Fig. 1(b)], which is then converted into a mechanical power. The experimentally observed threshold and linewidth are very well predicted by our theory in both devices. In the lower finesse *device 1*, the experiment shows earlier onset of saturation than theory, possibly due to influence of the higher order terms in the Taylor expansion of the photothermal force. In the higher finesse *device 2*, the observed output power is larger than predicted, which can be explained by the fact that in a higher $Q$ cavity any small variation in laser wavelength can shift the position of the "quiescent" point away from the one used to minimize threshold and effectively increase the saturation power, furthermore, the coupling efficiency can vary between two devices by a small amount. Also, the oscillations in our device do not show a complicated, often multistable character observed in cantilevered designs [10,20] but are much closer to the almost linear characteristics of the phonon laser in [12]. This can be explained by the fact that our cavity length is much shorter ($L_C = 3$ $\mu$m) and we can keep the laser tuned to a single quiescent point.

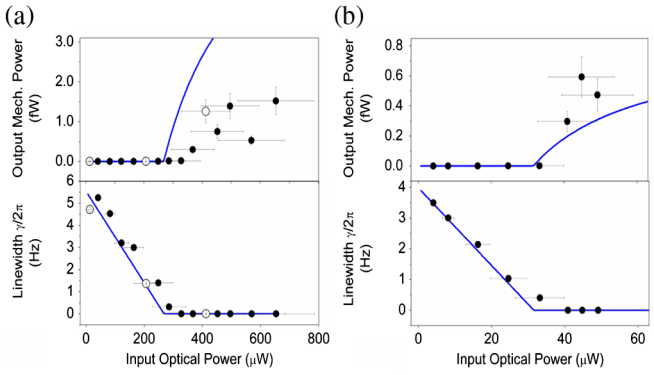


FIG. 2 (color online). Comparison of experimental (points) and theoretical (lines) results for two devices: (a) *device 1* output power and linewidth, (b) *device 2* output power and linewidth. The open data points in (a) correspond to the measured spectra shown in Fig. 1(b).

We now describe "phonon lasing" on a quantum level. The majority of optomechanical oscillators in which phonon lasing has been demonstrated are driven by radiation pressure and can be explained in the framework of Raman or Brillouin lasers: a parametric process in which the stimulated decay of a higher frequency photon creates a quantum of mechanical oscillation and a lower frequency (Stokes) photon in the cavity. [7,12]. But the situation is far more involved when the driving force is of a photothermal nature [5,10] and the interaction is mediated by a sequence of processes taking place inside the medium. The lasing can occur with either a blue- or a redshifted pump (the latter being the case in our experiments) a fact that cannot be explained by conventional parametric and Raman-like processes.

The parametric explanation can be obtained on the microscopic level by noticing that the thermal expansion driving the oscillating mechanical object is a consequence of the anharmonicity of the binding forces in the crystalline lattice. It is precisely this anharmonicity that engenders the three-phonon quantum interactions, specifically the process in which a higher-energy thermally excited acoustic phonon $\omega_p$ can split into two lower energy phonons. Here, one is the phonon of the mechanical oscillating mode with frequency $\omega_0$("signal" phonon), while the other one is the thermal "idler" phonon with frequency $\omega_p - \omega_0$ as shown in Fig. 3. The correspondence between the phonon anharmonicity and the second order optical nonlinearity is well established [21]. Hence, one can think of the oscillations as an "acoustic parametric oscillator". It is critical that the "pump" and idler phonons remain locked in phase with each other for all phonon modes $\omega_p$ since the light inside the optical cavity is modulated by the mechanical oscillations of one of the mirrors as $\cos(\omega_0 t)$ The number

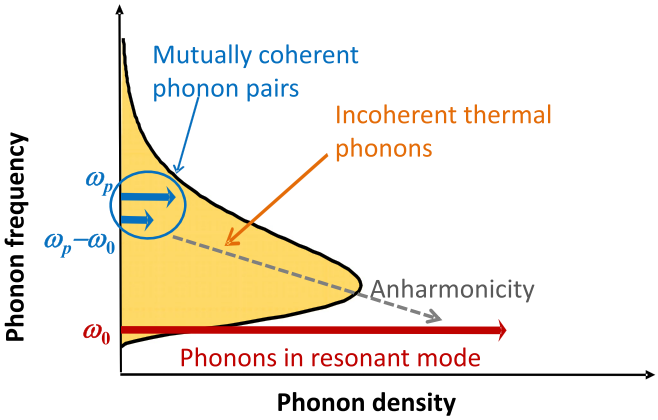


FIG. 3 (color online). The lasing cycle in the photothermal oscillator: the oscillating mechanical mode modulates the optical power in the cavity and the temperature establishing a phase coherence ($\omega_p$ and $\omega_p - \omega_0$) between some of the otherwise thermally incoherent phonons. Coherent phonons at the difference frequency $\omega_0$ are generated in the resonant mechanical mode via anharmonicity.

of photogenerated phonons is then modulated as $\cos(\omega_0 t + \varphi)$, and this modulation can be interpreted as interference between the phonons $\omega_p$ and phonon sidebands $\omega_p \pm \omega_0$ whose phases are coherently related. When $\varphi = \pi/2$, [strong quadrature component in Eq. (1)], a buildup of coherent "signal" oscillations will result in a manner similar to that of an optical parametric oscillator [22]. There is no need for all the thermal phonons at different frequencies $\omega_p$ to be coherent among themselves. It is quite sufficient to have a relatively small fraction of these phonons separated by the signal frequency $\omega_0$ to be locked in a phase relationship imposed by the oscillations of optical power. It is the energy of these pairs, $U_{\mathrm{st}}$ that plays the role of the energy stored at the upper level of the conventional laser.

This analogy easily explains the reasons for a low efficiency. First of all, only a small fraction of all the phonons are the coherently locked ones. Second, in each three-phonon process the average pump photon of THz frequency creates less than a MHz frequency coherent phonon—essentially a Manley-Rowe limit in nonlinear optics [22].

In conclusion, we have developed a set of phonon rate equations to describe self-oscillation in optomechanical systems. In analogy to the laser rate equations, our theory predicts a threshold optical power resulting in a linewidth narrowing and eventual linewidth collapse with a strong linear increase in oscillation amplitude. The agreement with experimental results (threshold power and slope efficiency) is very good indicating that self-oscillation in optomechanical systems can be described as a mechanical lasing process in which a pump (optical input) generates coherent acoustic phonons (mechanical output) via second order nonlinear phonon interactions. The collapse of the mechanical resonance linewidth and resulting strong increase in the effective mechanical $Q$ factor is of interest for sensing applications, where a large $Q_m$ leads to an increased sensing resolution.

The authors acknowledge support from the ASEE Summer Faculty Research program (J. B. K.) and the Office of Naval Research (M. W. P, T. H. S., and W. S. R). They also thank the NRL Nanoscience Institute staff for assistance with device fabrication.

[1] T. J. Kippenberg and K. J. Vahala, Science **321**, 1172 (2008).
[2] I. Favero and K. Karrai, Nature Photon. **3**, 201 (2009).
[3] F. Marqardt and S. M. Girvin, Physics **2**, 40, 2009.
[4] D. K. Armani, T. J. Kippenberg, S. M. Spillane, and K. J. Vahala, Nature (London) **421**, 925 (2003).
[5] C. H. Metzger and K. Karrai, Nature (London) **432**, 1002 (2004).
[6] S. Gigan, H. R. Böhm, M. Paternostro, F. Blaser, G. Langer, J. B. Hertzberg, K. C. Schwab, D. Bäuerle, M. Aspelmeyer, and A. Zeilinger, Nature (London) **444**, 67 (2006).
[7] O. Arcizet, P.-F. Cohadon, T. Briant, M. Pinard, and A. Heidmann, Nature (London) **444**, 71 (2006).
[8] A. Schliesser, P. Del'Haye, N. Nooshi, K. J. Vahala, and T. J. Kippenberg, Phys. Rev. Lett. **97**, 243905 (2006).
[9] T. J. Kippenberg, H. Rokhsari, T. Carmon, A. Scherer, and K. J. Vahala, Phys. Rev. Lett. **95**, 033901 (2005).
[10] M. Ludwig, C. Neuenhahn, C. Metzger, A. Ortlieb, I. Favero, K. Karrai, and F. Marquardt, Phys. Rev. Lett. **101**, 133903 (2008).
[11] K. Vahala, M. Hermann, S. Knunz, V. Batteiger, G. Saathoff, T. W. Hansch, and T. Udem, Nature Phys. **5**, 682 (2009).
[12] I. S. Grudinin, H. Lee, O. Painter, and K. J. Vahala, Phys. Rev. Lett. **104**, 083901 (2010).
[13] A. E. Siegman, *Lasers* (University Science Books, Sausalito, CA, 1986).
[14] H. Statz and G. De Mars, in *Quantum Electronics*, edited by C. H. Townes (Columbia University Press, New York, 1960), p. 530.
[15] D. A. Kleiman, Bell Syst. Tech. J. **43**, 1505 (1964), http://www.alcatel-lucent.com/bstj/vol43-1964/articles/bstj43-4-1505.pdf.
[16] M. W. Pruessner, T. H. Stievater, J. B. Khurgin, and W. S. Rabinovich, Opt. Express **19**, 21904 (2011).
[17] See Supplemental Material at http://link.aps.org/supplemental/10.1103/PhysRevLett.108.223904 for details of the derivation.
[18] M. Vogel, C. Mooser, K. Karrai, and R. J. Warburton, Appl. Phys. Lett. **83**, 1337 (2003).
[19] B. C. Johnson and A Mooradian, Appl. Phys. Lett. **49**, 1135 (1986).
[20] F. Marquardt, J. G. E. Harris, and S. M. Girvin, Phys. Rev. Lett. **96**, 103901 (2006).
[21] B. C. Daly, T. B. Norris, J. Chen, and J. B. Khurgin, Phys. Rev. B **70**, 214307 (2004).
[22] Y. R. Shen, *The principles of nonlinear optics* (Wiley, New York, 1984), Chap 9.